JME

Journal of Mining & Environment,
Published online: 26 June 2017.
DOI: 10.22044/jme.2017.931

Application of perfect mixing model for simulation of vertical roller mills

H. Shahgholi[1], K. Barani[1*] and M. Yaghobi[2]

1. Department of Mining Engineering, Lorestan University, Khorramabad, Iran
2. Nahavand Cement Company, Nahavand, Iran

Received 13 February 2017; received in revised form 18 May 2017; accepted 24 May 2017
**Corresponding author: barani.k@lu.ac.ir (K. Barani).*

Abstract
Vertical roller mills (VRMs) are well-established grinding equipment for various tasks in the coal and cement industry. There are few studies on simulation of VRMs. In this research work, application of perfect mixing model for simulation of a VRM in a cement grinding plant was investigated. Two sampling surveys were carried out on the VRM circuit. The samples and data from the first survey were used for the experimental determination of the breakage function and model calibration. The breakage distribution function of the material was determined by the compressed bed breakage test in a piston-die cell device. The model parameters were back-calculated using the feed and product size distribution data and the breakage distribution function. The model parameters obtained were used for simulation of the second survey and validation of the model. The simulation results showed that the simulated product size distribution curves fitted the measured product curves quite well.

Keywords: *Vertical Roller Mill, Grinding, Modeling, Simulation, Perfect Mixing Model.*

1. Introduction

Energy consumption during the raw mix and cement grinding process in a cement plant is the most critical issue that has been debated till now as 90% of the energy consumed and lost as heat and noise energy. The strategies against the rising energy consumption can be split in two groups: first, to avoid comminution, and secondly, to use a more efficient comminution technology. The application of vertical roller mills (VRMs) for ore grinding is a part of the second strategy [1].

In the mid 90's, LOESCHE introduced its VRMs with the 2+2-technology for grinding clinker and slag [2].

The grinding parts of a Loesche mill are illustrated in Figure 1 [1]. Several characteristics of VRMs are advantageous for the challenges in ore industry, especially in comparison with the conventional grinding technology. First of all, the particles are ground in a particle bed; the bed breakage is more energy-efficient and usually causes a narrower particle size distribution [3, 4]. Additionally, the crushing events are predominantly generated by particle-particle-contacts or phase–phase-contacts [5]. Both breakage modes have a selective effect, enhancing the liberation of the valuable mineral phases. The downstream processes benefit from the mentioned product characteristics of a VRM, which may lead to further improvements in the beneficiation process [1]. Due to a dry grinding process, no process water is required. However, a disadvantage of VRMs is the vibration of the rolls. Fujita and Saito [6] have determined that the mill vibration is caused by the frictional characteristics.

Modelling a grinding facility is an effective approach for process optimization. There are few studies on simulation of VRMs [7].

Wang et al. [7] have simulated the grinding process in vertical roller mills using a matrix model. It was based upon the actual experimental data obtained on cement clinker and coal grinding lines and from lab experiments. The pressure breakage function, B, was determined from the

laboratory test data with a hammer device. Pressure was applied to the hammer, and the breakage function matrix was obtained by size analysis of the broken particles. The breakage function and the selection function, in the form of a matrix, were used to numerically estimate the size distribution of the product. However, in the paper, it is unclear that the selection functions, S, was obtained from the test data, back calculation or literatures. According to the results obtained, there are more than one breaking stages in roller mills.

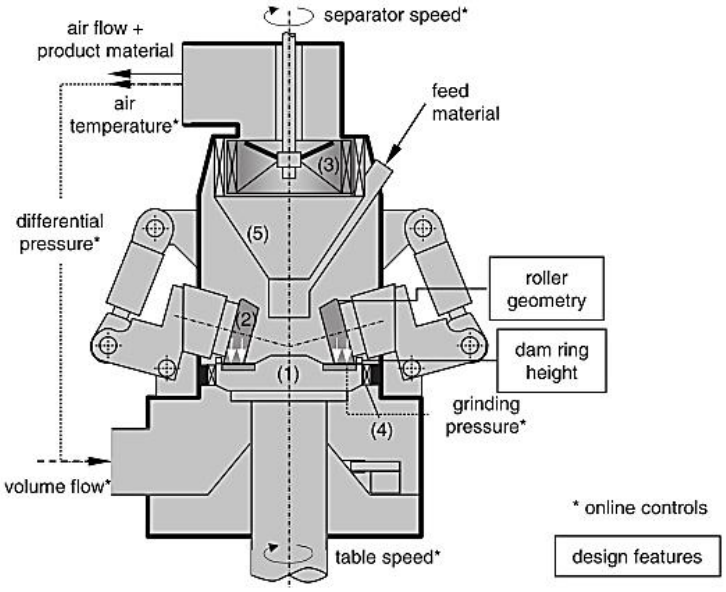

Figure 1. Schematic operation principle of a VRM [1].

Faitli and Czel [8] have used the matrix model for simulation of a VRM with high-efficiency slat classifier. On-site operational tests were performed in OMYA's limestone processing plant in Eger, Hungary, on a technology with Pfeiffer's 2800 C vertical roller grinding mill. The B breakage matrices were simply determined by the well-known Broadbent-Calcott function. A systematic test was carried out to grind the limestone samples in a laboratory Hardgrove mill to verify this assumption. The selection matrix, S, and number of breaking stages, v, were determined by the iterative computer simulation processing using the measured data.

Palaniandy et al. [9] have studied the optimization, modeling, and simulation of VRM in a cement raw mix grinding circuit with the Perfect mixing ball mill model. A series of samplings were conducted around the raw mix grinding circuit, and clinker samples were taken. The data obtained from the plant sampling was fitted with the perfect mixing ball mill model using the steady state mineral processing software, the JKSimmet. The breakage function and the breakage rate function for VRM were determined during the model fitting process. The Broadbent and Callcott equation was used as the breakage function. It was found that raw mix grinding in a VRM could be described by the perfect mixing model. In a perfect mixing ball mill, the feed entering the mill would be distributed along the mill, thus being subjected to the probability for breakage. A similar situation was encountered in a VRM, where the feed that had fallen on the grinding table was being subjected to the breakage process by the rollers, and the entire particles would have some probabilities for breakage.

The aim of this work was to simulate VRM using the perfect mixing model. Different from a previous work [9], the breakage functions were determined by laboratory breakage tests in a piston-die cell device. The data obtained from the plant sampling and breakage functions determination were fitted with the perfect mixing ball mill model using Excel spread sheet, and the other model parameters were back-calculated.

2. Perfect mixing model

The perfect mixing model has been developed on the assumption that the mill contents are perfectly mixed and the mill can be represented by one perfectly mixed segment or a number of perfectly mixed segments in series [10]. In the steady state operation, therefore, a mass balance forms the basis of the model, i.e.:

Feed + material broken from larger particles = material selected for breakage in the mill + material discharged

These parameters can be evaluated in the following way [10]:

1. Feed rate, denoted by the matrix F .
2. Removal rate for breakage, $R.s$, where R is a diagonal matrix giving the breakage rate of each component of the mill contents, s (for any component i, the rate of breakage is $R_i.s_i$). The mill contents matrix, s, represents the mass of the mill contents retained in each size fraction.
3. Appearance rate, denoted by $A.R.s$, where A is the appearance matrix.
4. Discharge rate, denoted by $P = D.s$, where D is a triangular matrix giving the fractional rates at which the components of the mill are discharged. For a perfectly mixed mill, the product will be the same as the mill contents. However, classification within the mill may occur, particularly for grate discharge mills, and hence, the product from the mill includes D and s .

These factors are combined to obtain the rate of change of mill contents:

$$\frac{\partial \mathrm{s}}{\partial \mathrm{t}} = \mathrm{A.R.s} - \mathrm{R.s+F-P} \tag{1}$$

With substituting P = D.s

$$\frac{\partial \mathrm{s}}{\partial \mathrm{t}} = (\mathrm{A.R} - \mathrm{R} - \mathrm{D}).\mathrm{s} + \mathrm{F} \tag{2}$$

At steady state, the rate of change of mill contents is zero or $\frac{\partial \mathrm{s}}{\partial \mathrm{t}} = 0$

Hence, Eq. (2) would be:

$$(\mathrm{A.R} - \mathrm{R} - \mathrm{D}).\mathrm{s} + \mathrm{F} = 0 \tag{3}$$

Since $P = D.s$ or $s = D^{-1}.P$, we can substitute for s in Eq. (3). Simplifying the resulting equation, the mathematical model for ball mills may be written as:

$$\mathrm{P} = \mathrm{D.R}^{-1}\left(\mathrm{I} - \mathrm{A} + \mathrm{DR}^{-1}\right)^{-1}.\mathrm{F} \tag{4}$$

This perfect mixing model has been successfully used to simulate ball mill and rod mill operations. It can be used for steady the state and dynamic simulations of the milling processes.

It is possible to evaluate Eq. (3), provided that the model parameters A, R, and *D* are known. The parameters R and D , however, are interdependent, and can only be determined if data on the mill contents is available. This is not always known in industrial mills. This may be overcome by lumping the two together as a combined parameter $D.R^{-1}$.

In order to evaluate the model parameters, assuming a steady state condition, rearrange Eq. (3) and substitute

$s = D^{-1}.P$:

$$0 = F + (A.R - R - D).D^{-1}.P = \tag{5}$$
$$F + A.R.D^{-1}.P - R.D^{-1}.P - P$$

or $F - P = (I - A).R.D^{-1}.P$ (6)

or $P = D.R^{-1}.(I - A)^{-1}.(F - P)$ (7)

From Eq. (1):

$$R.s = (I - A)^{-1}.(F - P) \tag{8}$$

and hence,

$$P = D.R^{-1}.R.s \tag{9}$$

Eq. (8) can be solved if the inverse of $(I - A)$ is known but this is seldom available. However, Eqs. (8) and (9) are two simultaneous equation in $R.s$. Both of these equations are triangular matrix equations, and can be solved using the back substitution technique. To use this technique, the equations have to be arranged in the matrix form:

$$\begin{bmatrix} (I-A_{11}) & 0 & 0 & \cdots & 0 \\ -A_{21} & (I-A_{22}) & 0 & \cdots & 0 \\ -A_{31} & -A_{32} & (I-A_{33}) & \cdots & 0 \\ \vdots & \vdots & \vdots & \ddots & 0 \\ -A_{n1} & -A_{n2} & -A_{n3} & \cdots & (I-A_{nn}) \end{bmatrix} . \begin{bmatrix} (R.s)_1 \\ (R.s)_2 \\ (R.s)_3 \\ \vdots \\ (R.s)_n \end{bmatrix} = \begin{bmatrix} (F_1 - P_1) \\ (F_2 - P_2) \\ (F_3 - P_3) \\ \vdots \\ (F_n - P_n) \end{bmatrix} \tag{10}$$

Expanding $(1-A_{11}).(R.s)_1=(F_1-P_1)$ (11)

or

$$(R.s)_1=\frac{(F_1-P_1)}{(1-A_{11})} \quad (12)$$

and

$$-A_{21}.(R.s)_1+(1-A_{22}).(R.s)_2=(F_2-P_2) \quad (13)$$

from which,

$$(R.s)_2=\frac{(F_2-P_2)+A_{21}.(R.s)_1}{(1-A_{22})} \quad (14)$$

The general solution can, therefore, be written as:

$$(R.s)_i=\frac{(F_i-P_i)\sum_{j=1}^{i=1}A_{ij}.(R.s)_i}{(1-A_{ii})} \quad (15)$$

$(R.s)_i$ can then be substituted in Eq. (9) to calculate $(D.R^{-1})$. If the size distribution of the mill contents is known, then the discharge matrix can be calculated from $P=D.s$; the rate of breakage matrix, R, can be determined from $(D.R^{-1})$.

For overflow mills and most of the operational range of grate discharge mills, the discharge elements can be approximated by:

$$D=\left[\frac{4V}{D^2L}\right]D^* \quad (16)$$

D^* is a diagonal matrix that is independent from size unless classification at the mill discharge occurs. D^* has diagonal values near unity. The combined parameter $(D.R^{-1})$ varies with the feed rate, and:

$$D.R^{-1}=\frac{4V}{D^2L}(D.R^{-1})^* \quad (17)$$

3. Experimental

3.1. Sampling

All the samples used in the lab experiments were taken from the clinker grinding line of Nahavand cement plant, Hamadan province, Iran. In the grinding line, the clinker was fed into VRM (LOESCHE mill) with a capacity of 120t/h (95% passing 30 mm). In the LOESCHE mill, the inter-particle comminution takes place in a material-filled gap between the rotating flat grinding table and the 4-conical grinding rollers. After comminution, the particles leave the table over its edge, and are taken up by an air stream to the dynamic high efficiency classifier incorporated in the casing of the mill. Particles meeting the product size leave the mill with the air, while the reject is fed back to the table for further comminution together with the fresh feed. The finished ground material leaves the mill after passing through the rotating cage of the classifier and is collected in a filter. From there, it is discharged and stored in silos for later transport to the downstream stages of processing.

Two surveys were carried out on the grinding circuit. The data collected from the first survey was used for modeling and simulation of the circuit, and the second survey was used for validation of the model parameters. For any survey, samples weighing 200 kg were collected from conveyor feed belt and the internal air classifier product over a period of two hours with 10 minutes interval. As taking sample from the internal classifier was impossible and the classifier had a role similar to an internal grate in the ball mill, the classifier product was considered as the VRM product.

The samples were riffled and sized by screening (for +0.5 mm particles) and laser size analyses (for -0.5 mm particles). Figure 2 shows the size distribution of the feed and product of VRM.

For grinding tests, the feed samples were carefully sieved to obtain the narrow size fractions. Seven narrow size fractions (-30 + 25 mm, -25 + 19.5 mm, -19.5 + 12.7 mm, -12.7 + 9.5 mm, -9.5 + 6.3 mm, -6.3 + 4mm, and -4 + 1.2 mm) were prepared from the feed sample.

3.2. Bed-breakage tests

The breakage distribution function of the material was determined by the well-explored lab-scale compressed bed breakage test in a piston-die cell device. The plan of the compressed bed-breakage tests is given in Figure 3. In this test, a small sample of materials is put in a cylindrical chamber. A piston is then forced on the materials with a press.

The test has been extensively used in the literature to model the bed-breakage grinding [3, 11-15]. Also the test has been used for modeling compression grinding in HPGR [16-18].

In the piston-die compression tests, the diameter of a die determines the top size of feed and the maximum pressure. A big die can accommodate large feed particles but applies a lower maximum

pressure. A low pressure means a low energy input. Sometimes a high energy input (a high pressure) is required for the competent rocks [18]. In order to cater for these two scenarios, 2 sets of piston-die devices were manufactured with diameters of 100 mm and 50 mm (Figure 4). The diameters for the pistons were 90 mm, and 46 mm. The height of the cylindrical chambers was set to 200 mm. Based upon the required pressure, both piston die cells were used for all fractions.
The amount of sample used in a piston die test work to simulate the breakage in a VRM has to comply with the following criteria:

- The amount of sample taken must not only be enough to represent a full size distribution expected at industrial scale but also to absorb efficiently the energy input.
- The compressed sample thickness should be similar to the VRM operating.

In order to map the breakage behavior of the material, seven narrow size fractions were compressed at different applied pressures. In the tests design, the experiences of other researchers and the operational pressure of VRM at the Nahavand cement plant (about 200 Mpa) were considered. However, the applied pressure was increased until a significant increase was not observed in the percent passing of one tenth of the original mean particle size particle for the ground material. The details of the size fractions and applied pressure levels are given in Table 1.

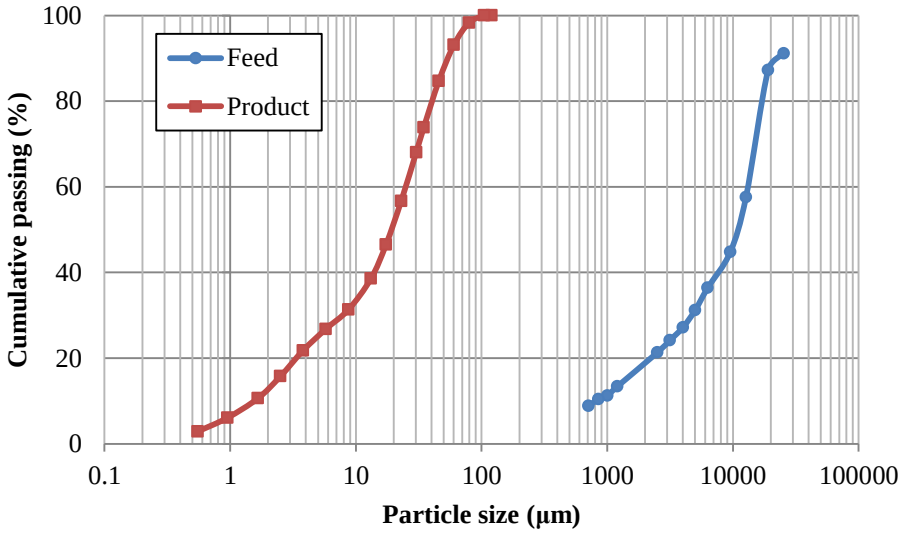

Figure 2. Particle size distribution of feed and product of VRM.

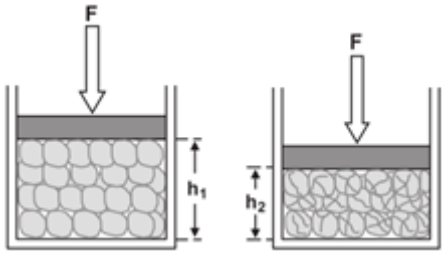

Figure 3. Representation of particle bed compression [16].

Figure 4. Piston-die cells.

Table 1. Bed-breakage tests on narrow size fraction samples.

Size fraction	Applied pressure (Mpa)
-38.1 + 25 mm	3.1,5.1
-25 + 19.5 mm	3.1, 5.1
-19.5 + 12.7 mm	3.1, 5.1, 20.4, 50.9, 101.9, 152.8, 203.8
-12.7 + 9.5 mm	3.1, 5.1, 20.4, 50.9, 101.9, 152.8, 203.8
-9.5 + 6.3 mm	3.1, 5.1, 20.4, 50.9, 101.9, 152.8, 203.8
-6.3 + 4 mm	5.1, 20.4, 50.9, 76.4, 101.9, 114.6, 152.8, 203.8
-4 + 1.2 mm	5.1, 20.4, 50.9, 76.4, 101.9, 114.6, 152.8, 203.8

4. Results and discussion

4.1. Breakage distribution function

After each test was completed, the resulting fragments were collected and sieved to give a product size distribution. The measured size distribution was then used to determine the breakage functions for the material.

The data evaluation for the compression breakage results was carried out using an evaluation method developed for single particle impact breakage tests by Narayanan [19]. The analytical procedure is based upon the assumption that the product size distributions are a function of the input energy or specific comminution energy (Ecs, $\frac{kWh}{t}$, hear applied pressure Mpa).

According to this method, the size distributions of the compressed materials were determined by a series of size distribution parameters such as $t_2, t_4, t_{10}, t_{25}, t_{50}$, and t_{75}, correspondingly expressing the cumulative percent passing size of $\frac{x}{2}, \frac{x}{4}, \frac{x}{10}, \frac{x}{25}, \frac{x}{50}$, and $\frac{x}{75}$, where x is the geometric mean of the size fractions. Figure 5 shows $t_2, t_4, t_{10}, t_{25}, t_{50}$, and t_{75} against t_{10}. Figure 5 is a useful graph. Each vertical line (or value of t_{10}) represents a complete size distribution, expressed as cumulative weight percent passing.

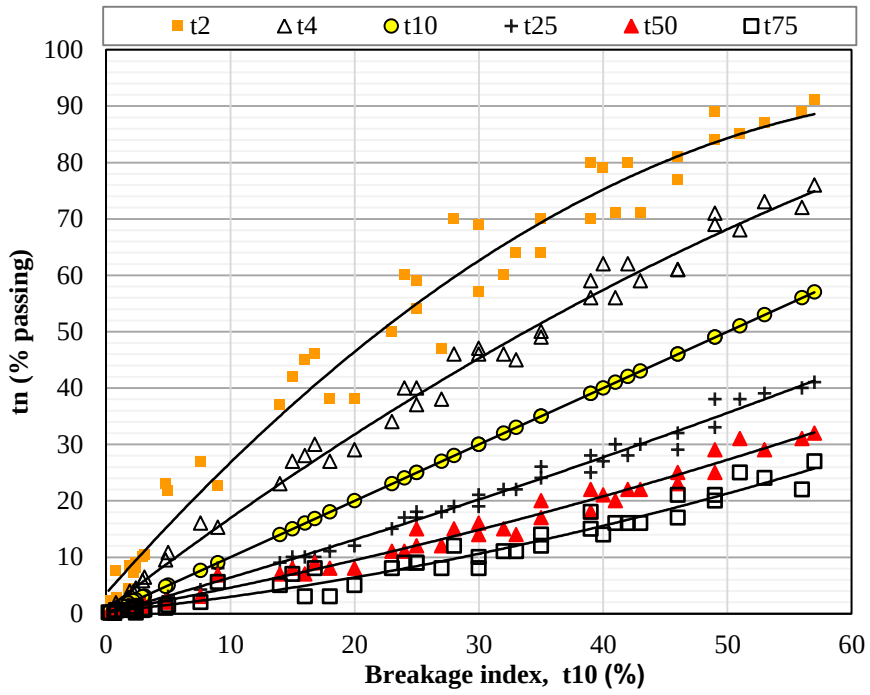

Figure 5. t_n *vs.* degree of breakage, t_{10}.

Since the product size is a function of the energy applied on to the parent size, Narayanan [19] defined a relationship between the specific comminution energy and product fineness for impact breakage data.

$$t_{10} = A \times (1 - e^{-b \times E_{cs}}) \quad (18)$$

where A and b are the material constants, and E_{cs} is the specific comminution energy (here, is applied pressure). A typical $E_{cs} - t_{10}$ relationship obtained from compressed bed-breakage tests is given in Figure 6. In this figure, the experimental results for different-size fraction at different-applied pressure (41 pairs $E_{cs} - t_{10}$) were fitted to Eq. (18), and then the relationship between the energy level and the product size distribution was obtained. Using this relationship, the breakage distribution was calculated for a given energy level. In the modeling approach presented here, the breakage distribution function was calculated for an applied pressure of 200 Mpa.

From Figure 6, and Eq (18), $t_{10} = 49.81\%$ was obtained for an applied pressure of 200 Mpa. In the following, $t_2, t_4, t_{10}, t_{25}, t_{50}$, and t_{75} were determined from Figure 5.

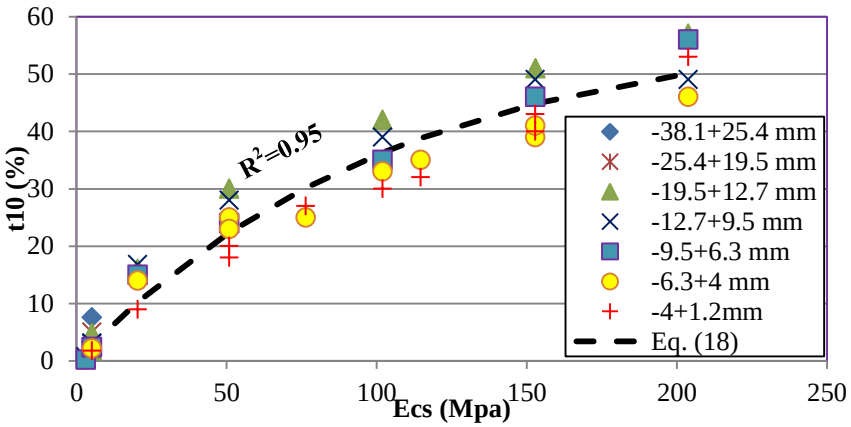

Figure 6. $E_{cs} - t_{10}$ **relationship.**

In the feed and product size distribution of VRM, there are a wide range of particle sizes from 25 mm to 10 µm (Figure 2). For application of the perfect mixing model and to obtain valid results, the breakage distribution function should be extended since the breakage distribution function obtained from Figure 5 was known just at 6 points. The values for t_n were fitted by Eq. (19) [20].

$$B_{i,1} = \varphi R^{\gamma} + (1-\varphi)R^{\beta} \qquad (19)$$

where R is relative size ($R = \frac{x_i}{x_1}$; for example, for t_2 value, $R = \frac{1}{2} = 0.5$) and φ, γ, and β are the characteristics of the material being ground and define the size distribution. These parameters were determined by plotting the B_{i1} (or t_n) values *vs.* the relative size (R) on log–log scales (Figure 7).

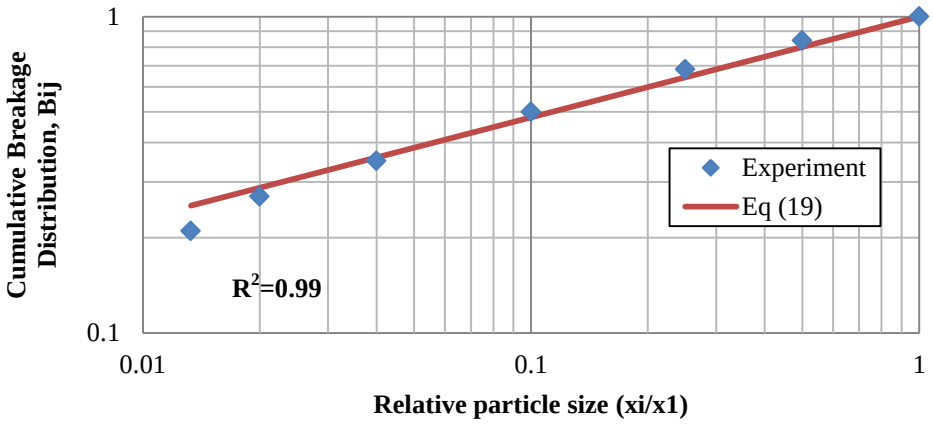

Figure 7. Cumulative breakage distribution function.

4.2. Model calibration

The Rosin-Rammler particle size distribution function was fitted to the feed and product size distribution from Figure 2, and the mathematical feed and product size distributions for 32 size classes were determined (column 3 and 4 in Table 2). From Eq (8) and using the breakage distribution function as a triangular matrix and feed and product distribution in a matrix form, $(R.s)_i$ was calculated as a diagonal matrix (column 6 in Table 2). $(R.s)_i$ was then substituted in Eq. (9), and $(D.R^{-1})_i$ was calculated as a diagonal matrix. Now, the model parameters are known and the mill product can be simulated using Eq (4). All calculation were done in Microsoft Excel.

4.3. Validation of model

Sampling data from the second survey was used for validation of the model parameters. The grinding condition such as the feed rate, operating pressure, and other mill setting parameters were

the same as the first survey. Thus it was assumed that the $(R.s)_i$ and $(D.R^{-1})_i$ parameters were not changed. Figure 8 shows the simulation results. It could be seen that the size distribution of the simulated product fitted well on the measured product (coefficient of determination or R-squared = 0.98), and the model gave a good prediction.

Table 2. Model fitting results.

Sieve number (i)	Sieve size (µm)	Mass retained (%)		Breackage function (b_{i1})	$(R.s)_i$	$(D.R^{-1})_i$
		Feed	Product			
1	25400	16.190	0.000	0.000	16.190	0.000
2	19050	8.734	0.000	0.088	10.151	0.000
3	12700	13.788	0.000	0.111	16.465	0.000
4	9525	9.761	0.000	0.070	13.461	0.000
5	6300	12.729	0.000	0.090	17.900	0.000
6	5000	6.158	0.000	0.046	12.022	0.000
7	4000	5.229	0.000	0.041	11.815	0.000
8	3150	4.831	0.000	0.041	11.488	0.000
9	2500	3.967	0.000	0.037	11.028	0.000
10	1200	8.798	0.000	0.100	16.965	0.000
11	1000	1.479	0.000	0.021	9.840	0.000
12	850	1.137	0.000	0.018	10.081	0.000
13	710	1.085	0.000	0.019	9.570	0.000
14	120.23	4.932	1.567	0.138	14.227	0.110
15	104.71	0.143	0.992	0.008	8.835	0.112
16	79.43	0.236	3.216	0.015	7.561	0.425
17	60.26	0.183	5.103	0.013	4.841	1.054
18	45.71	0.141	6.924	0.012	3.188	2.172
19	34.67	0.109	8.314	0.011	0.628	13.233
20	30.20	0.045	4.483	0.005	3.063	1.464
21	22.91	0.074	9.203	0.010	-2.109	-4.364
22	17.38	0.057	9.035	0.009	-2.765	-3.268
23	13.18	0.044	8.424	0.008	-2.055	-4.100
24	8.71	0.048	10.950	0.011	-6.351	-1.724
25	5.75	0.032	8.704	0.010	-5.079	-1.714
26	3.80	0.022	6.603	0.009	-3.966	-1.665
27	2.51	0.015	4.857	0.007	-2.117	-2.295
28	1.66	0.010	3.494	0.007	-1.906	-1.833
29	0.96	0.009	3.130	0.008	-1.534	-2.041
30	0.55	0.005	1.942	0.006	-1.055	-1.841
31	0.14	0.005	2.180	0.012	-1.407	-1.549
32	0.12	0.000	0.105	0.001	0.248	0.422

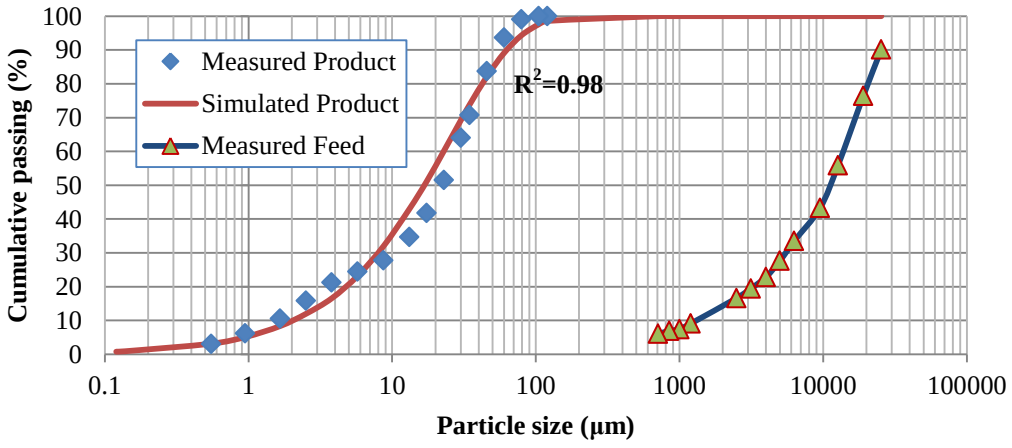

Figure 8. Comparison between simulated and measured product size distributions.

5. Conclusions

The perfect mixing model was used for simulation of a cement grinding vertical roller mill (VRM) based upon the survey data. The breakage distribution functions of the material were determined with the compressed bed breakage test in a piston-die cell device. The results obtained showed that the data from the breakage tests could be evaluated very well with the analytical procedure that was developed for single particle impact breakage tests. The simulation results show that the simulated product size distribution curves fit the measured product curves quite well. It can be concluded that the grinding process of a VRM is very well-predictable with the perfect mixing model.

However for a proper use of the perfect mixing model for VRM simulation, as shown in Eq (17) for ball mill, a further research work is required to determine the relation between the discharge rate (D), volumetric feed rate, and dimensions of VRM.

Acknowledgments

The authors would like to thank Nahavand Cement Plant and Lorestan University for funding this research work.

References

[1]. Reichert, M., Gerold, C., Fredriksson, A., Adolfsson, G. and Lieberwirth, H. (2015). Research of iron ore grinding in a vertical-roller-mill. Minerais Eng. 73: 109-115.

[2]. Schaefer, H.V.U. (2001). Loesche vertical roller mills for the comminution of ores and minerals. Miner. Eng. 14 (10): 1155-1160.

[3]. Viljoen, R.M., Smit, J.T., Du Plessis, I. and Ser, V. (2001). The development and application of in-bed compression breakage principles. Miner. Eng. 14 (5): 465-471.

[4]. Fuerstenau, D.W. (1992). Comminution: past developments, current innovation and future challenges. In Proceedings of the International Conference on Extractive Metallurgy of Gold and Base Metals. pp. 15-21.

[5]. Fandrich, R., Gu, Y., Burrows, D. and Moeller, K. (2007). Modern SEM-based mineral liberation analysis. Int. J. Miner. Process. 84: 310-320.

[6]. Fujita, K. and Saito, T. (2006). Unstable vibration of roller mills. J. Sound Vib. 297 (1): 329-350.

[7]. Wang, J.H., Chen, Q.R., Kuang, Y., Lynch, A.J. and Zhuo, J. (2009). Grinding process within vertical roller mills: experiment and simulation. Min. Sci. Technol. 19 (1): 97-101.

[8]. Faitli, J. and Czel, P. (2014). Matrix Model Simulation of a Vertical Roller Mill with High-Efficiency Slat Classifier. Chem. Eng. Technol. 37 (5): 779-786.

[9]. Palaniandy, S., Azizli, M. and Azizi, M.D.K. (2006). Optimization, Modeling and Simulation of Vertical Roller Mill in Cement Raw Mix Grinding Circuit. Universiti Sains Malaysia.

[10]. Gupta A. and Yan, D.S. (2016). Mineral processing design and operations: an introduction. 1st ed. Perth. Australia. Elsevier.

[11]. Aziz, J. (1980). Single-particle size reduction and bed loading conditions for cement clinker fractions. ZKG, Zement-Kalk-Gips, Ed. A. 33 (5): 213-218.

[12]. Fuerstenau, D.W., Gutsche, O. and Kapur, P.C. (1996). Confined particle bed comminution under compressive loads. Int. J. Miner. Process. 44: 521-537.

[13]. Oettel, W., Nguyen, A.Q., Husemann, K. and Bernhardt, C. (2001). Comminution in confined particle beds by single compressive load. Int. J. Miner. Process. 63 (1): 1-16.

[14]. Hosten, C. and Cimilli, H. (2009). The effects of feed size distribution on confined-bed comminution of quartz and calcite in piston-die press. Int. J. Miner. Process. 91 (3): 81-87.

[15]. Barrios, G.K.P., de Carvalho, R.M. and Tavares, L.M. (2011). Modeling breakage of monodispersed particles in unconfined beds. Miner. Eng. 24 (3): 308-318.

[16]. Dundar, H., Benzer, H. and Aydogan, N. (2013). Application of population balance model to HPGR crushing. Miner. Eng. 50-51: 114120.

[17]. Esnault, V.P.B., Zhou, H. and Heitzmann, D. (2015). New population balance model for predicting particle size evolution in compression grinding. Miner. Eng. 73: 7-15.

[18]. Kalala, J.T. (2011). Using piston die tests to predict the breakage behavior of HPGR. In 5th International Conference Autogenous and Semi-Autogenous Grinding.

[19]. Narayanan, S.S. (1986). Single particle breakage tests: a review of principles and application to comminution modeling. Bull. Proc. Austr. Inst. Min. Met. 291 (4): 49-58.

[20]. Austin, L.G., Klimpel, R.R. and Luckie, P.T. (1984). Process Engineering of Size Reduction: Ball Milling. SME-AIME New York. USA.

شبیه‌سازی آسیاهای غلتکی عمودی با استفاده از مدل مخلوط کامل

حسین شاهقلی[1]، کیانوش بارانی[1*] و محسن یعقوبی[2]

۱- بخش مهندسی معدن، دانشگاه لرستان، ایران

۲- شرکت سیمان نهاوند، ایران

ارسال ۲۰۱۷/۲/۱۳، پذیرش ۲۰۱۷/۵/۲۴

* نویسنده مسئول مکاتبات: barani.k@lu.ac.ir

چکیده:

اخیراً استفاده از آسیاهای غلتکی عمودی در مدار خردایش صنایع سیمان و زغال‌سنگ متداول شده است. با این وجود، تحقیقات اندکی در زمینه شبیه‌سازی این آسیاها انجام شده است. در این تحقیق شبیه‌سازی یک آسیای غلتکی عمودی در مدار یک کارخانه سیمان با استفاده از مدل مخلوط کامل مورد بررسی قرار گرفته است. برای این منظور دو مرحله پیمایش و نمونه‌گیری بر روی مدار خردایش صورت گرفته است. اطلاعات و نمونه‌های گرفته شده در پیمایش اول برای تعیین توابع توزیع شکست و کالیبراسیون مدل مورد استفاده قرار گرفته است. توابع توزیع شکست در آزمایشگاه با آزمون شکست لایه‌ای و در یک پیستون سیلندر تعیین شده‌اند. پارامترهای مدل با کمک اطلاعات توزیع دانه‌بندی خوراک و محصول و توابع توزیع شکست به روش محاسبات برگشتی تعیین شده‌اند. پارامترهای مدل برای شبیه‌سازی پیمایش دوم و همچنین اعتبارسنجی مدل مورد استفاده قرار گرفته‌اند. نتایج شبیه‌سازی نشان داد که نمودار توزیع دانه‌بندی محصول شبیه‌سازی شده برازش بسیار خوبی بر روی توزیع دانه‌بندی محصول واقعی دارد.

کلمات کلیدی: آسیای غلتکی عمودی، آسیا کنی، مدل‌سازی، شبیه‌سازی، مدل مخلوط کامل.